Optica Applicata, Vol. XXXIV, No. 2, 2004

Thermal models for silicon-on-insulator-based optical circuits

KONRAD BIWOJNO, SŁAWOMIR SUJECKI, ANA VUKOVIC, TREVOR M. BENSON, PHIL SEWELL

School of Electrical and Electronic Engineering, University of Nottingham, University Park, Nottingham NG7 2RD, UK

Silicon has many advantages as a material for planar photonics but it does not possess a linear electro-optic effect. Whilst free carrier injection has been used to produce optical switches based on silicon on insulator (SOI) rib waveguides, the thermo-optic effect provides an attractive alternative way of modulating the refractive index in these structures. In this paper a fast analytical thermal solver is developed for SOI-based thermo-optic switches. It is shown that lateral heat leakage limits the temperature rise that can be achieved for a given thermal input power. The analytical model is then extended to allow investigation of the effect of thermal isolation trenches. These are found to improve performance by a factor of three. Finally, the effect of these trenches on the modes supported by the waveguide is briefly discussed.

Keywords: thermo-optic switch, silicon-on-insulator, rib waveguide.

1. Introduction

Silicon is a very attractive material for optoelectronics because of the availability of high quality wafers, a mature processing technology and the material's high index of refraction, [1]–[3]. Many industrially important optical devices have been demonstrated in silicon-on-insulator (SOI) material, which is characterised by small optical losses and full compatibility with CMOS technology. These include both basic elements (such as low-loss optical rib waveguides for 1.3 to 1.5 μm wavelengths and single-mode rib waveguides with dimensions comparable with single-mode optical fibres [4]–[6]) and sophisticated components for advanced applications (such as multiplexers, demultiplexers, optical attenuators and add-drop filters) [7]–[14].

Switching is a key element of flexible optical communication systems. Since silicon is centro-symmetric it does not possess a linear electro-optic effect. Optical switches and variable optical attenuators based on free carrier injection have been reported in SOI waveguides. An alternative physical phenomenon to modulate the refractive index in silicon-based structures is the thermo-optic effect. The thermo-optic effect results from the fact that the materials' refractive indices are temperature dependent, *i.e.*, a change in temperature causes a change in the refractive index.

Thermo-optic switches can potentially provide low transmission loss, high stability, low power consumption and suitability for very large scale integration. These attractive features mean that much effort is pushed towards the development of thermo-optic switches, not only in SOI waveguides but also in silicon-oxynitride-based [15] and polymer-based [16] photonic circuits. Thermo-optically-controlled active waveguide components including tunable Bragg grating filters, optical add-drop multiplexers, tunable arrayed waveguide gratings and digital optical switches have all been reported in the recent literature.

In this paper we present an analytical thermal analysis for a thermo-optic switch based on a SOI rib waveguide. A metal heater deposited over the rib generates the thermal energy. By controlling the electrical power applied to the heater the temperature profile inside the structure, and hence the associated changes in local refractive index within the waveguide, can be calculated. These changes in the refractive index result in the required phase shift of the guided optical signal, which can be readily calculated using a numerical approach such as the finite difference (FD) method [17]. Results obtained show that lateral heat leakage limits the temperature rise that can be achieved for a given thermal input power. A modified design, incorporating a trench etched into the silicon remote from the rib region is also investigated and shown to improve the performance of the modulator within a photonic integrated circuit.

2. Initial theory: simple SOI rib waveguide modulator design

Consider Figure 1 which shows the cross-section of a SOI rib waveguide with a metal heater deposited over the rib and a perfect heat-sink at the bottom of the silicon substrate. It is required to solve the heat flow equation $\nabla \cdot K \nabla T = 0$ [18] (where the heat flow per unit area is given by $Q = -K\nabla T$ and K is the thermal conductivity), subject to $-K\nabla T = Q_{\mathrm{inc}}(x)$ on top of rib where $Q_{\mathrm{inc}}(x)$ is a known heat flow

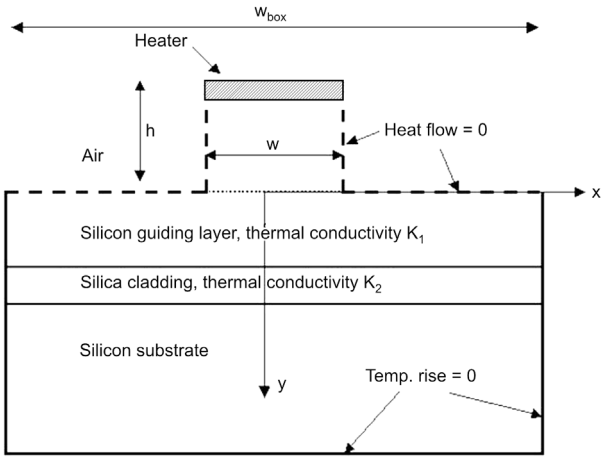

Fig. 1. Thermo-optic modulator based on SOI rib waveguide.

distribution. It can be assumed that there is no heat flow into the air cladding region since the thermal conductivity of air (0.32 $Wm^{-1}K^{-1}$ at 100 °C) is much smaller than that of silicon and silica [19].

The temperature $T(x, y)$ in both the rib ($y < 0$) and substrate ($y \geq 0$) regions can be expressed as a superposition of the local separable solutions of the governing equation. In the rib ($y < 0$) we write:

$$T(x, y) = \sum_{n = 0, 1} \cos\left(\frac{n\pi x}{w}\right)\left[T_n \cosh\left(\frac{n\pi(y + h)}{w}\right) - \frac{Q_n}{K_1(n\pi/w)} \sinh\left(\frac{n\pi(y + h)}{w}\right)\right] \tag{1}$$

so that

$$\begin{aligned} T(x, -h) &= \sum_{n = 0, 1} \cos\left(\frac{n\pi x}{w}\right) T_n, \\ Q_y(x, -h) &= \sum_{n = 0, 1} \cos\left(\frac{n\pi x}{w}\right) Q_n = Q_{\text{inc}}(x). \end{aligned} \tag{2}$$

Just below the rib we can write

$$\begin{aligned} T(x, y) &= \sum_{p = 0, 1} \cos(s_p x)\, t_p \left[\frac{\exp(-s_p y) + R_p \exp(+s_p y)}{1 + R_p}\right], \\ s_p &= \frac{(2p + 1)\pi}{2w_{\text{box}}}, \end{aligned} \tag{3}$$

$$Q_y(x, y) = K_1 \sum_{p = 0, 1} \cos(s_p x)\, t_p s_p \left[\frac{\exp(-s_p y) - R_p \exp(+s_p y)}{1 + R_p}\right], \tag{4}$$

where R_p is the p-th spectral "reflection coefficient" seen looking down into the multi-layered substrate referred to $y = 0$ and Q_y is the vertical heat flow. Explicitly matching Q_y at the base of the rib, noting that this is zero for $|x| > w/2$

$$[Y_p s_p K_1] t_p = \frac{2}{w_{\text{box}}} \sum_{n = 0, 1} P_{pn}\left[-T_n K_1\left(\frac{n\pi}{w}\right) \sinh\left(\frac{n\pi h}{w}\right) + Q_n \cosh\left(\frac{n\pi h}{w}\right)\right] \tag{5}$$

where $P_{pn} = \int_0^w \mathrm{d}x \cos(s_p x) \cos\left(\frac{n\pi x}{w}\right)$ and $Y_p = \frac{1 - R_p}{1 + R_p}$.

Now, match the temperature T over the base of the rib ($|x| < w/2$) in a Galerkin sense to give:

$$\alpha_m \left(T_m \cosh\left(\frac{m\pi h}{w}\right) - \frac{Q_m}{K_1(m\pi/w)} \sinh\left(\frac{m\pi h}{w}\right) \right)$$

$$= \frac{2}{w_{\text{box}}} \sum_{n=0,\,1} \sum_{p=0,\,1} \frac{P_{pm} P_{pn}}{s_p K_1 Y_p} \left[- T_n K_1\left(\frac{n\pi}{w}\right) \sinh\left(\frac{n\pi h}{w}\right) + Q_n \cosh\left(\frac{n\pi h}{w}\right) \right] \tag{6}$$

where for $\alpha_m = w/2$ for $m \neq 0$ and $\alpha_0 = w$ for all p. This can be expressed as a matrix equation, solvable for T, $\underline{\underline{A}}\,\underline{T} = \underline{E}$, where

$$A_{mn} = \alpha_m \delta_{mn} \cosh\left(\frac{m\pi h}{w}\right) + \frac{2}{w_{\text{box}}} \sum_{p=0,\,1} \frac{P_{pm} P_{pn}}{s_p Y_p} \left(\frac{n\pi}{w}\right) \sinh\left(\frac{n\pi h}{w}\right), \tag{7}$$

and

$$E_m = \alpha_m \frac{Q_m}{K_1(m\pi/w)} \sinh\left(\frac{m\pi h}{w}\right) + \frac{2}{w_{\text{box}}} \sum_{n=0,\,1} \sum_{p=0,\,1} \frac{P_{pm} P_{pn}}{s_p K_1 Y_p} Q_n \cosh\left(\frac{n\pi h}{w}\right). \tag{8}$$

2.1. Results for simple modulator design

Numerical results are presented for an SOI waveguide modulator with a total silicon guiding layer thickness of 5 μm and a rib height (etch depth) of 1.7 μm. The rib width is 4 μm, the silica cladding layer thickness is 0.4 μm and the silicon substrate thickness is 500 μm. The thermal conductivity of silicon was taken to be 150 $\text{Wm}^{-1}\text{K}^{-1}$ and that of silica 1 $\text{Wm}^{-1}\text{K}^{-1}$ [19]. An applied power of 1 W per centimetre length of device is assumed, uniformly distributed across the heater. Convergence of the method was observed with increasing the number of expansion terms in both rib and substrate terms. Figure 2 demonstrates the convergence of T_0, the uniform term in the expansion of the temperature at the top of the rib, with the number of expansion terms in the rib, for a box width of 200 μm. The T_0 term represents the average temperature rise at the top of the rib, since the other terms in the expansion average to zero. Calculation times were typically eight seconds on a Pentium III 833 MHz PC. The width of the outer box w_{box} has a noticeable effect on the temperature at the top of the rib T_0 even for values of w_{box} of the order of 1000 μm, as shown in Fig. 3. This is because significant horizontal heat flow occurs. This not only limits the temperature rise that can be

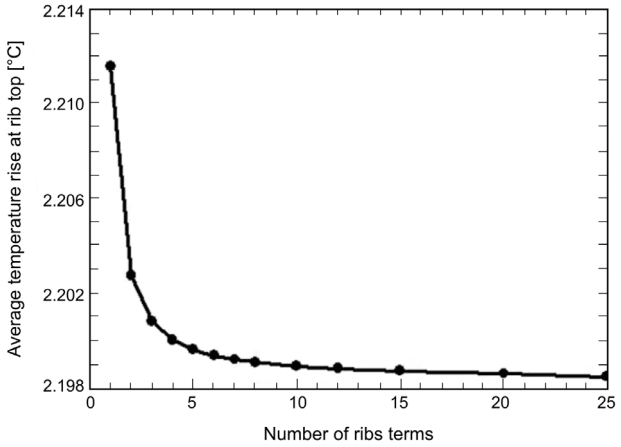

Fig. 2. Convergence of T_0, the uniform term in the expansion of the temperature at the top of the rib, with the number of expansion terms in the rib for a 4 μm wide rib etched to a depth of 1.7 μm. The box width is 200 μm and 1 $\mathrm{Wcm^{-1}}$ is applied to the rib heater.

achieved in the modulator for a given heater power but will also have an undesirable effect on other devices fabricated on the same single substrate. Furthermore, although numerical methods such as the finite difference method, lend themselves to the study of thermal problems the significant lateral heat flow away from the rib in the silicon guiding layer makes accurate truncation of the workspace hard to achieve for this particular structure [20]. It was found that as w_{box} was allowed to extend to infinity results asymptotically approached those obtained using the true Fourier transform (*i.e.*, the unboxed solution).

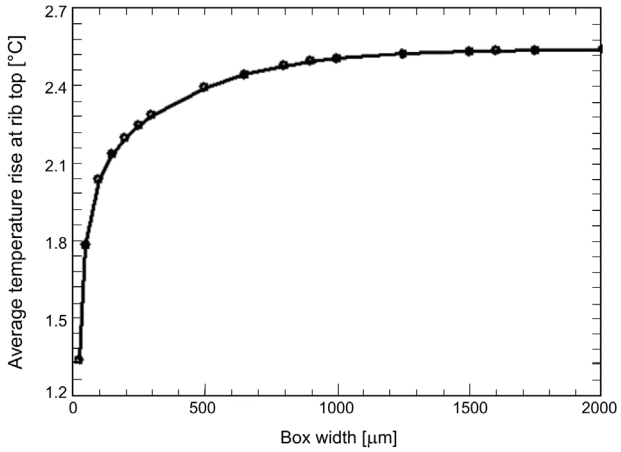

Fig. 3. Convergence of T_0, the average temperature rise at the top of the rib, with box width. 1 $\mathrm{Wcm^{-1}}$ is applied to the rib heater. The rib is 4 μm wide and etched to a depth of 1.7 μm. The box width is 200 μm.

3. Theory for modified modulator design including thermal isolation trenches

Results presented in the previous section show that lateral heat leakage in the modulator presented in Fig. 1 limits the temperature rise that can be achieved for a given thermal input power. Furthermore this heat leakage means that very large transverse separations will be needed to thermally isolate such a thermo-optic modulator from any adjacent devices. A modified design, incorporating a trench etched into the silicon remote from the rib region (Fig. 4) was therefore investigated and shown to improve the performance of the modulator within a photonic integrated circuit. Consider now the modified modulator design presented in Fig. 4 which incorporates two trenches of depth d symmetrically located about the rib. The edges of each trench are at $|x| = x_1$ and $|x| = x_2$.

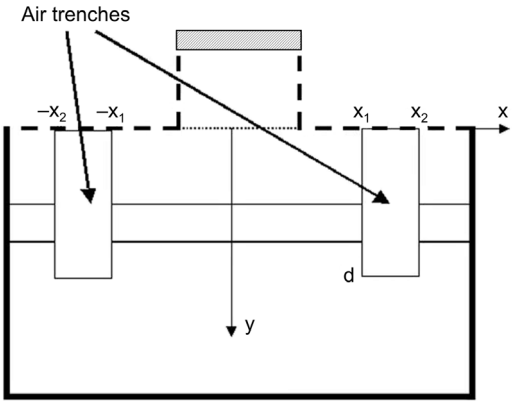

Fig. 4. Modified modulator design including thermal isolation trenches.

Let $G(x, y; x', y')$ be the Green's function, defined as a solution to $\nabla \cdot K \nabla G = -\delta(x - x')\,\delta(y - y')$ and satisfying the temperature and heat flow boundary conditions between layers in the substrate as well as $\mathrm{d}G/\mathrm{d}y = 0$ at $y = 0$. Let there be a single layer potential on the contour enclosing the trench, except on the top where $y = 0$. Let c parametrically define this contour, which is of length L and express the single layer potential as

$$\Phi = \sum_{u\,=\,0,\,1} \phi_u \cos\left(\frac{u\pi c}{L}\right). \tag{9}$$

Then the single layer potential gives rise to the following temperature and heat flow

$$T = \int_0^L \mathrm{d}c' G(x, y; x', y') \Phi(x', y'),$$
$$Q = -K(x, y) \nabla \int_0^L \mathrm{d}c' G(x, y; x', y') \Phi(x', y'). \tag{10}$$

We choose to add these solutions to those arising from the sources in the rib described in Sec. 2.1. Given that $\mathrm{d}G/\mathrm{d}y = 0$ at $y = 0$, explicitly matching Q_y at the base of the rib is performed as above. Define a transfer function that gives the normal heat flow at a point (x, y), which lies on the trench boundary due the injected Q_y at the base of the rib

$$\hat{n}(x, y) Q(x, y) = \sum_{p = 0, 1} \cos(s_p x)\, t_p Y(s_p; y). \tag{11}$$

Proceeding as before, T is matched at the base of the rib. We now have an additional term arising from the trench single layer potential such that:

$$T_m \cosh\left(\frac{m\pi h}{w}\right) - \frac{Q_m}{K_1(m\pi/w)} \sinh\left(\frac{m\pi h}{w}\right)$$
$$= \frac{2}{w_{\mathrm{box}}} \sum_{n = 0, 1} \sum_{p = 0, 1} \frac{P_{pm} P_{pn}}{s_p K_1 Y_p} \left[- T_n K_1\left(\frac{n\pi}{w}\right) \sinh\left(\frac{n\pi h}{w}\right) + Q_n \cosh\left(\frac{n\pi h}{w}\right) \right]$$
$$+ \sum_{u = 0, 1} \sum_{p = 0, 1} \int_0^w \mathrm{d}x \cos\left(\frac{m\pi x}{w}\right) \int_0^L \mathrm{d}c' G(x, y; x', y')\, \phi_u \cos\left(\frac{u\pi c'}{L}\right). \tag{12}$$

We also require that Q_n, the normal heat flow into the trench is zero, hence

$$\int_0^L \mathrm{d}c \cos\left(\frac{v\pi c}{L}\right) \left[\sum_{p = 0, 1} \cos(s_p x) t_p Y(s_p; y) \right.$$
$$\left. - K(x, y) \frac{\partial}{\partial n} \int_0^L \mathrm{d}c' G(x, y; x', y') \phi_u \cos\left(\frac{u\pi c'}{L}\right) \right] = 0 \tag{13}$$

for all v. Hence overall we have the matrix equation

$$\begin{bmatrix} \underline{\underline{A}} & \underline{\underline{B}} \\ \underline{\underline{C}} & \underline{\underline{D}} \end{bmatrix} \begin{bmatrix} \underline{T} \\ \underline{\phi} \end{bmatrix} = \begin{bmatrix} \underline{E} \\ \underline{F} \end{bmatrix} \tag{14}$$

where A and E are defined as above and

$$B_{mu} = -\sum_{p=0,1} \int_0^w \mathrm{d}x \cos\left(\frac{m\pi x}{w}\right) \int_0^L \mathrm{d}c' G(x, y; x', y') \phi_u \cos\left(\frac{u\pi c'}{L}\right), \tag{15}$$

$$C_{vn} = \int_0^L \mathrm{d}c \cos\left(\frac{v\pi c}{L}\right) \frac{2}{w_{\mathrm{box}}} \sum_{p=0,1} \cos(s_p x) P_{pn} \frac{Y(s_p; y)}{s_p Y_p} \frac{n\pi}{w} \sinh\left(\frac{n\pi h}{w}\right), \tag{16}$$

$$D_{vu} = \int_0^L \mathrm{d}c \cos\left(\frac{v\pi c}{L}\right) K(x, y) \frac{\partial}{\partial n} \int_0^L \mathrm{d}c' G(x, y; x', y') \cos\left(\frac{u\pi c'}{L}\right), \tag{17}$$

$$F_v = \int_0^L \mathrm{d}c \cos\left(\frac{v\pi c}{L}\right) \frac{2}{w_{\mathrm{box}}} \sum_{n=0,1} \sum_{p=0,1} \cos(s_p x) P_{pn} \frac{Y(s_p; y)}{s_p K_1 Y_p} \frac{n\pi}{w} \cosh\left(\frac{n\pi h}{w}\right) Q_n. \tag{18}$$

In a multi-layered substrate of infinite width the Green's function can be written as

$$G(x, y; x', y') = \frac{2}{\pi} \int_{-\infty}^{\infty} \mathrm{d}s \exp(-js(x - x')) g(s; y, y') \tag{19}$$

where $g(s; y, y') = \delta_{ij} g_0(s; y, y') + a_{ij}(y') \exp(sy) + b_{ij}(y') \exp(-sy)$. Here, the y and y' are in the i-th and j-th layers and the terms a_{ij} and b_{ij} ensure that the boundary conditions between the layers are satisfied, and

$$g_0(s; y, y') = \frac{\exp(-s|y - y'|)}{2sK(y')} \tag{20}$$

When evaluating the function $\frac{\partial}{\partial x} \int_0^L \mathrm{d}c' G(x, y; x', y') \Phi$ non-convergent integrals arise due to the term g_0 if the order of integration and differentiation is exchanged. This is overcome by recognising that

$$\frac{2}{\pi}\int_{-\infty}^{\infty} \mathrm{d}s \exp(-js(x-x'))\frac{\exp(-|s||y-y'|)}{2|s|}\,\mathrm{sgn}(s) \xrightarrow[x\to x']{} -\frac{\delta(y-y')\,\mathrm{sgn}(x-x')}{2} \tag{21}$$

allowing us to write

$$\frac{\partial}{\partial x}\int_0^L \mathrm{d}c'\, G(x,y;x',y')\,\Phi(c') = -\frac{\Phi(x,y)\,\mathrm{sgn}(x-x')}{2}$$

$$+\int_0^L \mathrm{d}c'\frac{2}{\pi}\int_{-\infty}^{\infty}\mathrm{d}s \exp(-js(x-x'))\left[\frac{\partial}{\partial x}g(s;y,y') + \frac{\delta(y-y')}{js}\right]\Phi(c') \tag{22}$$

given that $\frac{2}{\pi}\int_{-\infty}^{\infty}\mathrm{d}s\,\frac{\exp(-js(x-x'))}{js} = \frac{\mathrm{sgn}(x-x')}{2}$. This makes the integrals over s convergent.

3.1. Results for modified modulator design including thermal isolation trenches

Figure 5**a** shows the T_0, the uniform term in the expansion of the temperature at the top of the rib, as a function of trench depth d for a 0.5 μm wide trench positioned at $x_1 = 2$ μm and then $x_1 = 5$ μm. The presence of the trench can increase the temperature at the top of the rib by a factor of about three. However, it is also clear from Fig. 5 that a significant temperature rise does not occur until the trench is deep enough to enter the silica layer. Moreover, it is seen that moving the trench further away from the rib reduces the rise in temperature. Figure 5**b** shows that the width of the trench is not really significant. Figure 6 shows some typical temperature and heat flow distributions for a trench 3.5 μm deep, 0.5 μm wide and with $x_1 = 2$ μm that substantiate this behaviour.

3.2. Effect of thermal isolation trenches on optical properties of the modulator

The modulators studied have been based upon SOI rib waveguide structures that support only a single mode, despite the fact that the rib region is several microns wide and several microns high. These waveguides rely on a high optical leakage loss of higher order modes into the adjacent slab regions for their single mode behaviour [4], [5]. It might be expected that the presence of the etched trenches in the modified modulator design illustrated in Fig. 4 would affect this design. Finite difference

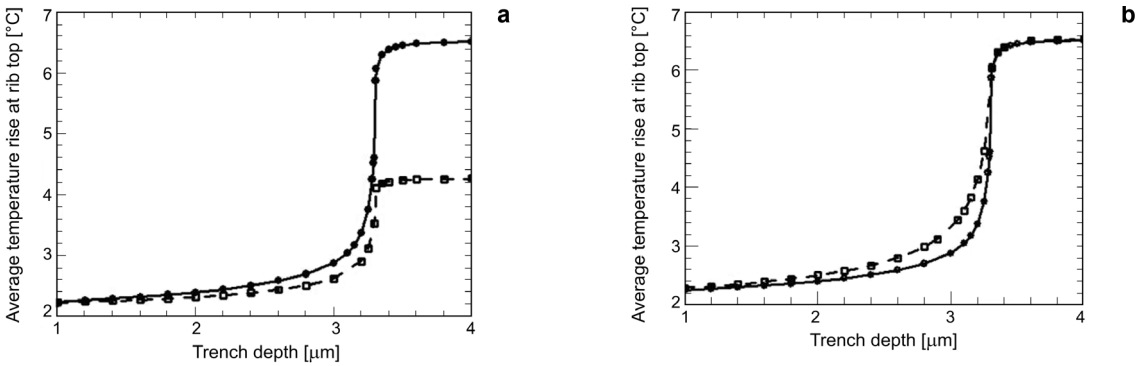

Fig. 5. Variation in T_0, the average temperature rise at the top of the rib, with trench depth d when 1 Wcm^{-1} is applied to the rib heater; **a** – 0.5 μm wide trenches positioned at x_1 = 2 μm (solid line) and 5 μm (dashed line); **b** – trenches 0.5 μm wide (solid line) and 2 μm wide (dashed line) positioned at x_1 = 2 μm. The box width is 200 μm.

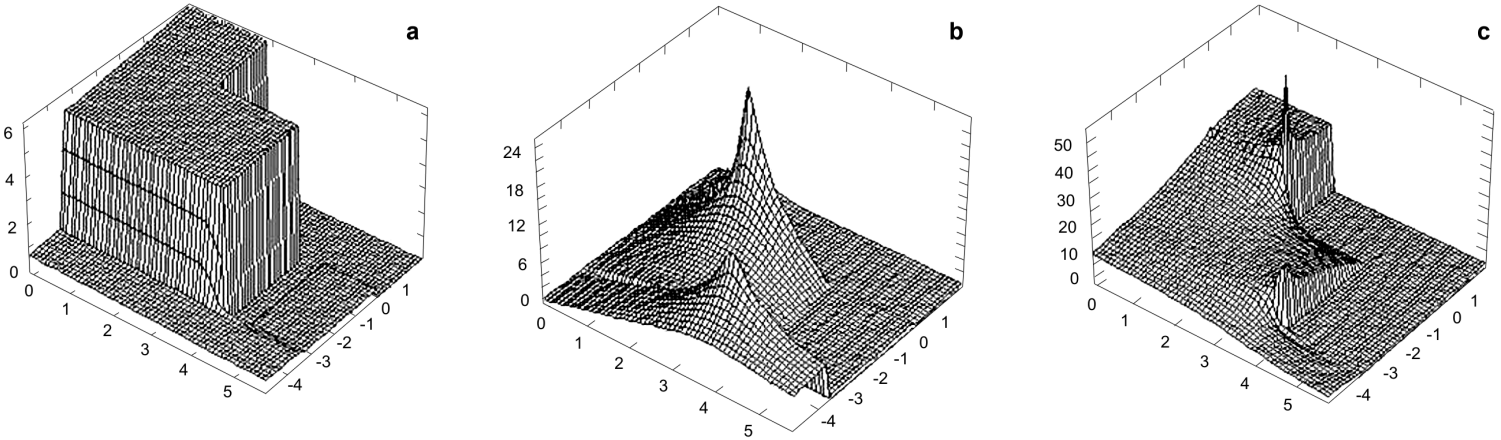

Fig. 6. Temperature profile (**a**), horizontal heat flow (**b**) and vertical heat flow (**c**) for a rib 4 μm wide and etched to a depth of 1.7 μm when 1Wcm^{-1} is applied to the rib heater. Trenches 0.5 μm wide and 3.5 μm deep are positioned at x_1 = 2 μm and the box width is 200 μm.

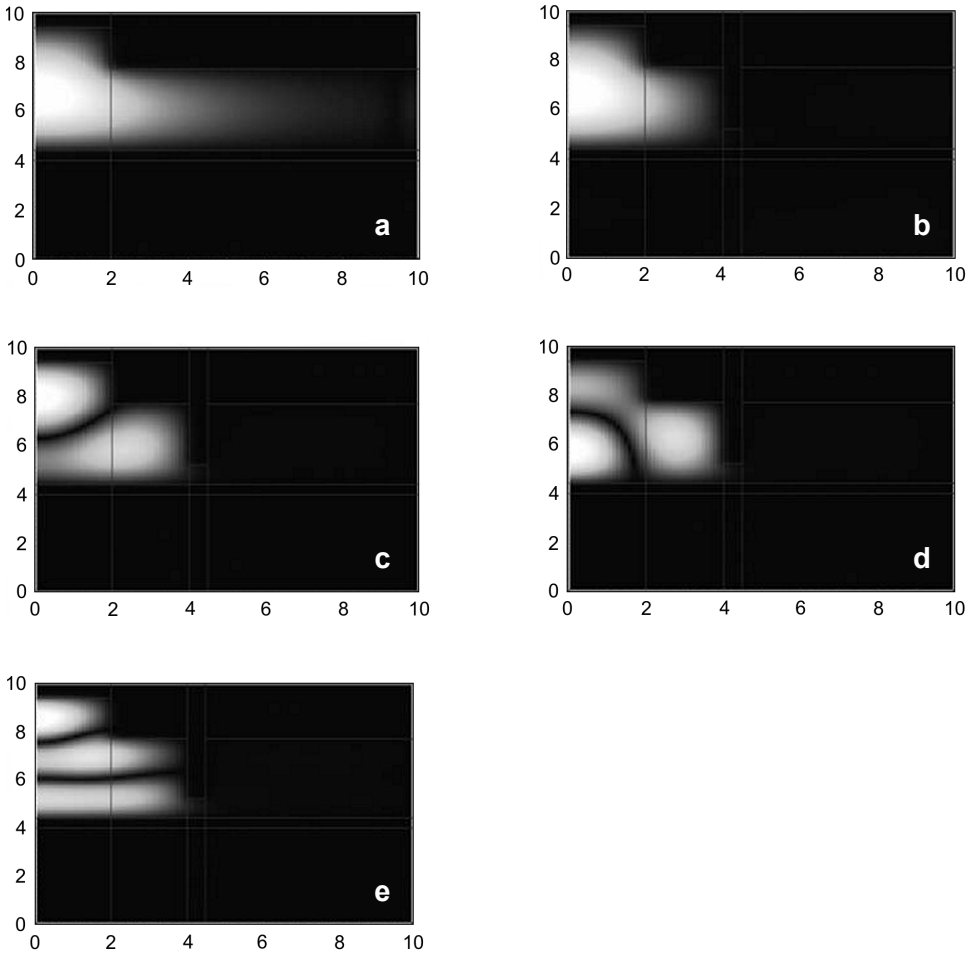

Fig. 7. Half-cross-section of guided mode profiles at a wavelength of 1.55 μm for fundamental mode supported by a 4 μm wide SOI rib waveguide with no thermal isolation trench (**a**) and fundamental and higher order modes in the structure when the thermal isolation trenches (**b**)–(**e**) are included.

simulations of the mode properties of the simple and modified modulator designs were undertaken. Figure 7**a** presents the modal profile of the fundamental mode supported by an SOI rib waveguide of width 4 μm at a wavelength of 1.55 μm with no thermal isolation trench. Figure 7**b**–**e** shows the fundamental and higher order modes in the structure when the thermal isolation trenches are included. The trenches are 2.5 μm deep and 0.5 μm wide and positioned at x_1 = 2 μm. It can be seen that whilst the trenches do not significantly perturb the fundamental mode the higher order modes become bound. Because the fundamental mode in the structure with and without trenches is very similar, careful design of the interface to the switch will minimise the derogatory effects of the higher order modes.

4. Conclusions

A fast analytical thermal solver has been described for the evaluation of thermo-optic modulators and switches based on a metal heater deposited on a SOI rib waveguides. The new solver enables thermal simulations to be run in a matter of seconds on a PC with minimal computer memory requirements. Results obtained using the solver have shown that lateral heat leakage limits the temperature rise that can be achieved for a given heater power. Furthermore, this leakage is likely to have an undesirable effect on adjacent devices even when device separation is of the order of 1000 μm. Thermal isolation trenches were incorporated into an extended model using a single layer potential. Although the inclusion of these trenches complicates the analysis, the simulation software maintains its speed and efficiency. The thermal isolation trenches can improve the temperature rise for a given thermal power by a factor of three and provide almost complete thermal isolation, as long as they are etched through the silica confinement layer.

Acknowledgments – The authors are grateful to Bookham Technology for their financial support of this project.

References

[1] SOREF R.A., LORENZO J.P., IEEE J. Quantum Electron. **QE-22** (1986), 873.
[2] SOREF R., MRS Bull., April (1998), 20.
[3] IEEE Journal of Selected Topics in Quantum Electronics, Special Issue on Silicon-based Optoelectronics, 4, no. 6, November/December 1998.
[4] SOREF R.A., SCHMIDTCHEN J., PETERMANN K., IEEE J. Quantum Electron. **27** (1991), 1971.
[5] SCHMIDTCHEN J., SPLETT A., SHUPPERT B., PETERMANN K., BURBACH G., Electron. Lett. **27** (1991), 1486.
[6] RICKMAN A.G., REED G.T., IEE Proc. Optoelectron. **141** (1994), 391.
[7] ZHAO C.Z., LI G.Z., LIU E.K., GAO Y., LIU X.D., Appl. Phys. Lett. **67** (1995), 2448.
[8] TRINH P.D., YEGNANARAYANAN S., COPPINGER F., JALALI B., IEEE Photonics Technol. Lett. **9** (1997), 940.
[9] LITTLE B.E., CHU S.T., HAUS H.A., FORESI J.S., LAINE J.P., J. Lightwave Technol. **15** (1997), 998.
[10] TRINH P.D., YEGNANARAYANAN S., JALALI B., Electron. Lett. 31, no.24, 1995, 2097.
[11] TRINH P.D., YEGNANARAYANAN S., JALALI B., IEEE Photonics Technol. Lett. **8** (1996), 794.
[12] TRINH P.D., YEGNANARAYANAN S., JALALI B., Technical Digest of Integrated Photonics Research **6** (1996), 273.
[13] JALALI B., YEGNANARAYANAN S., YOON T., YOSHIMOTO T., RENDINA I., COPPINGER F., IEEE Journal of Selected Topics in Quantum Electronics **4** (1998), 938.
[14] http://www.bookham.com/pages/products/productmenu.html
[15] HORST F., BEYELER R., BONA G-L., FLUSK E., GERMANN R., OFFREIN B., SALAMINK H., WIESMANN D., [In] *Proceedings Integrated Photonics Research*, Quebec 2000, p. 110.
[16] ELDADA L. NORMWOOD R., BLOMQUIST R., SHACKLETTE L.W., MCFARLAND M., [In] *Proceedings Optical Fiber Communication Conference*, Vol. 2, 2000, p. 124.

[17] STERN M.S., IEE Proc. Optoelectron. **135** (1988), 57.
[18] PATANKAR S.V., *Numerical Heat Transfer and Fluid Flow*, Hemisphere Publishing Corporation, New York 1980.
[19] LIDE D.R., *CRC Handbook of Chemistry and Physics: a Ready Reference Book of Chemical and Physical Data*, 81st edition, London 2000.
[20] BIWOJNO K., *Numerical analysis of thermal switching in silicon-based integrated optics devices*, M.Sc. Thesis, Kielce University of Technology, Poland, 2001.

Received June 23, 2003